Molecular Basis for *Bacillus thuringiensis* Cry1Ab Toxin Specificity: Two Structural Determinants in the *Manduca sexta* Bt-R_1 Receptor Interact with Loops α-8 and 2 in Domain II of Cy1Ab Toxin†

Isabel Gómez,‡ Donald H. Dean,§ Alejandra Bravo,‡ and Mario Soberón*,‡

Departamento de Microbiología Molecular, Instituto de Biotecnología UNAM, Apdo postal 510-3, Cuernavaca, Morelos 62250, México, and Department of Biochemistry, The Ohio State University, Columbus, Ohio 43210

Received March 18, 2003; Revised Manuscript Received July 10, 2003

ABSTRACT: The identification of epitopes involved in Cry toxin−receptor interaction could provide insights into the molecular basis of insect specificity and for designing new toxins to overcome the potential problem of insect resistance. In previous works, we determined that the *Manduca sexta* Cry1A cadherin-like receptor (Bt-R_1) interacts with Cry1A toxins through epitope ^{865}NITIHITDTNN^{875} and by loop 2 of domain II in the toxin (Gomez, I., Miranda-Rios, J., Rudiño-Piñera, E., Oltean, D. I., Gill, S. S., Bravo, A., and Soberón, M. (2002) *J. Biol. Chem. 277,* 30137−30143.). In this work, we narrowed to 12 amino acids a previously identified Bt-R_1 66 amino acids epitope (Dorsch, J. A., Candas, M., Griko, N. B., Maaty, W. S. A., Midbo, E. G., Vadlamudi, R. K., and Bulla, L. A., Jr. (2002) *Insect Biochem. Mol. Biol. 32,* 1025−1036) and identified loop α-8 of Cry1Ab domain II as its cognate binding epitope. Two amino acid Bt-R_1 toxin binding regions of 70 residues, one comprised of residues 831−900 containing the ^{865}NITIHITDTNN^{875} epitope (TBR1) and the other comprised of residues 1291−1360 (TBR2) were cloned by RT-PCR and produced in *Escherichia coli*. Cry1A toxins bind with the two TBR regions in contrast with the nontoxic Cry3A toxin. The loop 2 synthetic peptide competed with the binding of Cry1Ab toxin to both TBR regions in contrast to the α-8 synthetic peptide that only competed with Cry1Ab binding to TBR2. Western blots and competition ELISA analysis showed that the Cry1Ab loop 2 RR368-9EE mutant did not show observable binding to TBR1 but still bound the TBR2 peptide. This result suggests that loop α-8 interacts with the TBR2 region. Competition ELISA analysis of Cry1Ab binding to the two TBR peptides revealed that the toxin binds the TBR1 region with 6-fold higher affinity than the TBR2 region. The amino acid sequence of TBR2 involved on Cry1Ab interaction was narrowed to 12 amino acids, ^{1331}IPLPASILTVTV^{1342}, by using synthetic peptides as competitors for Cry1Ab binding to Bt-R_1. Our results show that the specificity of Cry1A involves at least two structural determinants on both molecules.

Bacillus thuringiensis (Bt)[1] is an agronomic important bacterium because of the production of insecticidal toxins (Cry proteins) during the sporulation process. Several Bt strains are used worldwide as alternative insecticides to control caterpillar, coleopterous, or vector mosquitoes. Moreover, recombinant DNA technology has yielded insect-resistant transgenic crop-plants (Bt-crops) that have been planted commercially for the past few years.

The proposed mode of action of Cry toxins involves solubilization of Cry protoxins, proteolytic activation, receptor binding, pre-pore formation, membrane insertion, and finally pore formation leading to cell swelling and lysis (*1*). Cry proteins are formed of three structural domains. The crystal structure of trypsin activated Cry1Aa (lepidopteran specific) Cry3A (coleopteran specific) and Cry2Aa (dipteran specific) protoxin have been solved (*2*−*4*). Seven α-helices form the N-terminal domain I that has been characterized as a part of the pore-forming activity. Domain III has also been implicated in pore formation (*5*−*7*). Domain II consists of three antiparallel β-sheets with exposed loop regions, and domain III is a β-sandwich (*2*−*4*). Domains II and III are involved in receptor recognition. In particular, loop regions of domain II are involved in receptor binding (for reviews, see refs *1*, *8*, and *9*).

The major concern regarding the use of Bt-crops is the generation of insect populations resistant to Cry toxins. Different mechanisms of insect resistance using laboratory-selected insect populations have been characterized (*10*−*15*). Among them, the most frequent mechanism has been the selection of insects affected on receptor−toxin interaction (*11*−*15*). Therefore, it is crucial to determine the molecular

† This work was partially supported by CONACyT Contract 27637-N and G36505-N; DGAPA-UNAM IN206200 and IN216300; UC MEXUS-CONACYT; and the United States Department of Agriculture, USDA, 2002-3502-1239. The work of D.H.D. is supported by a grant from the National Institutes of Health, R01 AI29092.

* Corresponding author. Tel: (52-777) 3291618. Fax: (52-777) 3172388. E-mail: mario@ibt.unam.mx.

§ The Ohio State University.

‡ Instituto de Biotecnología UNAM.

[1] Abbreviations: Bt-R_1, Cry1A cadherin-like receptor; TBR, toxin binding region; APN, aminopeptidase-*N*; Bt, *Bacillus thuringiensis*; scFv, single chain antibody fragment; BBMV, brush border membrane vesicles.

10.1021/bi034440p CCC: $25.00
Published on Web 08/13/2003

basis of Cry toxin−receptor interaction since this knowledge could be useful in designing new toxins that could overcome the potential generation of resistant insect populations in nature. Two lepidopteran Cry1A receptors have been identified as cadherin-like and aminopeptidase-*N* (APN) molecules (*16*−*22*). For both receptors, different experimental evidence suggest their involvement in toxicity (*12*, *19*, *23*−*29*). The binding affinity of APN is in the range of 100 nM (*26*), while that of cadherin-like receptors (Bt-R_1) is in the range of 1 nM (*18*). The differences of binding affinities between APN and Bt-R_1 suggest that binding to Bt-R_1 is the first event on the interaction of Cry1A toxins with microvilli membranes, and therefore, the primary determinant of insect specificity.

Regarding the receptor binding epitopes, in previous work we identified an scFv antibody (scFv73) that inhibited binding of Cry1A toxins to the cadherin-like receptor Bt-R_1, but not to APN, and reduced the toxicity of Cry1Ab to *Manduca sexta* larvae (*30*). Sequence analysis of the CDR3 region of scFv73 led to the identification of an eight amino acid epitope of the *M. sexta* cadherin-like receptor, Bt-R_1, (^{869}HITDTNNK^{876}), involved in binding with Cry1A toxins (*30*). Loop 2 of domain II of the Cry1A toxins was identified as the cognate binding epitope of the ^{869}HITDTNNK^{876} epitope (*31*). This finding highlights the importance of the ^{869}HITDTNNK^{876} binding epitope since extensive mutagenesis of loop 2 of Cry1A toxins has shown that this loop region is important for receptor binding and toxicity (*32*, *33*). Accumulating evidence indicates that proteins can interact through amino acid sequences displaying inverted hydropathic profiles (*34*). The interaction of loop 2 with the Bt-R_1 ^{869}HITDTNN^{875} region was shown to be determined by hydropathic complementarity and that the binding epitope (^{865}NITIHITDTNN^{875}) could be larger than the epitope identified by sequence similarity to scFv73 (*31*). Recently, a second Cry1A binding site in Bt-R_1 was mapped by heterologous expression of truncated derivatives (*27*). This region comprised 66 amino acids from residues 1296−1362 (*27*). This result suggests that toxin−receptor interactions involve several structural determinants on both molecules.

Mutagenesis studies have shown that besides domain II loop 2, loops α-8 and 3 of the Cry1A toxins are important for receptor interaction and toxicity (*32*, *33*, *35*−*38*). The Bt-R_1 epitopes involved in binding loops α-8 and 3 regions remain unidentified. In this paper, we show that loops 2 and α-8 of the Cry1Ab toxin have similar binding capabilities. Nevertheless, cloning two different truncated 70 residue peptides of Bt-R_1 corresponding to the two characterized toxin binding regions (TBR) and their characterization with respect to the binding to Cry1A toxins in the presence of different synthetic peptides as binding competitors demonstrated that loop 2 binds to the ^{865}NITIHITDTNNK^{876} region as previously reported (*31*), while loop α-8 binds to the region ^{1331}IPLPASILTVTV^{1342} in the Bt-R_1 receptor.

EXPERIMENTAL PROCEDURES

Bacterial Strains and Media. The acrystalliferus Bt strain 407 *cry*$^-$ transformed with pHT315 plasmid (*39*) harboring the *cry1Aa* gene or pHT315-1Ab harboring the *cry1Ab* gene (*30*) were used for Cry1Aa and Cry1Ab production, respectively. Cry1Ac was produced from wild-type Bt strain HD73. The transformant and wild-type strains were grown for 3 days at 29 °C in nutrient broth sporulation medium (*30*) supplemented with 10 μg/mL erythromycin only for Cry1Aa and Cry1Ab. Cry3A was isolated from sporulated Bt subsp. *tenebrionis* culture. Cry1Ab F371A and RR368-369EE mutant proteins were purified from *Escherichia coli* strains harboring the mutated genes.

Purification of Cry Toxins. The spores and crystals were harvested and washed with buffer containing 0.01% Triton X-100, 50 mM NaCl, and 50 mM Tris-HCl, pH 8.5. Crystals were purified by sucrose gradients as reported (*28*, *30*), solubilized at 37 °C for 2 h in extraction buffer (50 mM Na_2CO_3 pH 10.5, 0.2% β-mercaptoethanol), and then activated with trypsin (1:20 w/w) for 2 h at 37 °C. PMSF was added to a final 1 mM concentration to stop proteolysis. Samples were centrifuged at 16 000*g* for 10 min, and the toxin-containing supernatant was harvested. Cry3A was purified as reported (*40*), solubilized at 37 °C for 12 h in extraction buffer (50 mM Na_2CO_3 pH 10.5, 0.2% β-mercaptoethanol), and then activated with chymotrypsin (2:1 w/w) for 12 h at 37 °C. Cry1Ab mutants in *E. coli* were purified as previously described (*41*). The final pellet, referred to as the crystal protein, was solubilized in extraction buffer (50 mM Na_2CO_3 pH 10.5, 10 mM dithiothreitol) at 37 °C for 2 h. The solubilized protoxin was digested with trypsin (1:50 w/w) at 37 °C for 2 h.

Preparations of Brush Border Membrane Vesicles (BBMVs). *M. sexta* eggs were reared on an artificial diet. BBMVs from fifth instar *M. sexta* were prepared as reported except that neomycin sulfate (2.4 μg/mL) was included in the buffer (300 mM manitol, 2 mM dithiothreitol, 5 mM EGTA, 0.1 mM phenylmethylsulfonylfluoride, 150 μg/mL peptatin A, 100 μg/mL leupeptin, 1 μg/mL soybean trypsin inhibitor, 10 mM HEPES-HCl, pH 7.4) (*30*, *42*).

Toxin Overlay Assays. Protein blot analysis of BBMV preparations was performed as previously described (*30*, *31*). Cry1Ab toxin was biotinylated using biotinyl-*N*-hydroxysuccinimide ester (Amersham Pharmacia Biotech, Buckinghamshire, UK) and was visualized by incubating with a streptavidin-peroxidase conjugate. To determine the ability of peptides to compete with the Cry1Ab toxin, different concentrations of the peptides were incubated with biotinylated Cry1Ab toxin in washing buffer (0.1% Tween 20, 0.2% bovine albumin in phosphate-buffered saline) for 1 h at room temperature before adding the mixture to nitrocellulose membranes. Single gel-blots were incubated with different competitors using the PR 150 mini deca-probe (Amersham Pharmacia, Little Chalfont, UK) that was designed to incubate each lane of the blot in different conditions avoiding the need of cutting lanes for different conditions. Ten parallel troughs milled in one side of the upper plate became individual incubation chambers when the unit was assembled. Pure synthetic peptides (more that 90%) were purchased from invitrogen (Carlsbad, CA) and stored and reconstituted as suggested by the manufacturers. For hydrophobic peptides (L2-Ab, EpTBR2), 0.3% dimethyl sulfoxide was added for solubilization. Amino acid sequences of synthetic peptides used for competition experiments are shown in Table 1.

Western Blot of Cry1Ab Toxin. Activated toxin was separated in SDS−PAGE, transferred onto a nitrocellulose membrane PVDF, blocked with skimmed milk (5%), detected with anti-Cry1Ab polyclonal (1/80 000; 1 h), and visualized with a goat anti-rabbit antibody coupled with

Table 1: Synthetic Peptide Sequences

name	description	sequence
Lα-8	amino acid sequence of Cry1Ab loop α-8	SFRGSAQGIEGS
L2-Ab	amino acid sequence of Cry1Ab loop 2	RRPFNIGINNQQ
Scr	scramble amino acid sequence of scFv73 CDR3	SGRNSTSLV
BtR1−Cry	amino acid sequence of residues 869−876 of Bt-R_1	HITDTNNKAA
EpTBR2	amino acid sequence of residues 1331−1342 of Bt-R_1	IPLPASILTVTV
NonEpTBR2	amino acid sequence of residues 1296−1307 of Bt-R_1	LDPVRNRLFLKK

horseradish peroxidase (HRP) (Sigma, St. Louis, MO) (1/5000; 1 h), followed by SuperSignal chemiluminescent substrate (Pierce, Rockford, IL) as described by the manufacturers. Detection of Cry1Ab toxin with scFv73 antibody was performed as previously described (*30*, *31*). The membranes were then incubated in 200 nM scFv73 antibody, followed by anti-c-myc antibody (Sigma, St. Louis, MO) (1:5000 dilution), and then a secondary goat anti-mouse antibody conjugated with peroxidase (Sigma, St. Louis, MO) (1:5000 dilution). Blots were visualized using SuperSignal (Pierce, Rockford, IL) as described by the manufacturers. For competition experiments, TBR's peptides were incubated with different concentrations of synthetic peptides (Table 1) for 1 h at room temperature before incubating with Cry1A blots using the PR 150 mini deca-probe (Amersham Pharmacia, Little Chalfont, UK) as described above.

Toxicity Assays of Manduca sexta. Bioassays were performed with *M. sexta* neonate larvae using surface-treated food with 9 ng/cm^2 as reported (*30*, *31*), and mortality was recorded after 7 days.

Construction of Truncated Bt-R_1 Fragments, Cloning, and Expression. Total RNA was prepared from 3 g of midgut tissues from fifth instar *M. sexta* larvae using the acid guanidinium−phenol−chloroform method (*43*), and first strand c-DNA was generated using first strand cDNA synthesis Kit for RT-PCR (AMV) (Roche, Nutley, NJ), according to the manufacturer's instructions using specific primers for each region. For the first PCR reaction, each truncated Bt-R_1 fragment was amplified using Vent-Polimerase (New England BioLabs, Beverly, MA). For the TBR1 region, the primers used were TBRGIU:GACGCGGATACTCCTCCA and TBRGIL:AGTGACCACCTCGTCTAA; for the TBR2 region, the primers used were TBRBU:GATGGCAACAGCGAAGGT and TBRBL:TGTTGATATCCCTGCGGT. Two PCR products of 230 pb corresponding to TBR1 and TBR2 were obtained. In a second PCR reaction using the PCR products as template, restriction *SfiI* and *NotI* sites were incorporated by using the primers TBRGIUSFI: GAG AGA GAG AGA GAG AGA GAG GCC CAG CCG CCG ACG CGG ATA CTC CTC CA and TBRGILNOT: GAG AGA GAG AGA GAG AGA GAG CGG CCG CAG TGA CCA CCT CGT CTA for TBR1 and primers TBRBUSFI:GAG AGA GAG AGA GAG AGA GAG GCC CAG CCG GCC GAT GGC AAC AGC GAA GGT and TBRBLNOT:GAG AGA GAG AGA GAG AGA GAG CGG CCG CTG TTG ATA TCC CTG CGG T for TBR2. PCR products of 300 bp were purified with the QIAquick PCR Purification Kit (Qiagen, Valencia, CA) and digested with *SfiI* and *NotI* (New England BioLabs, Beverly, MA), ligated in the vector pSyn1 previously digested *SfiI* and *NotI* with poly-histidine and c-myc tagging and expression. Constructions were subsequently electroporated into *E. coli* TG1 cells. Peptide expression was performed as previously reported (*30*). His-tagged proteins were purified on a nickel affinity column as previously described (*30*).

Determination of TBR Peptide Affinities to Cry1Ab Toxin by Competition ELISA. To measure the kinetics of association of TBR peptides to Cry1Ab toxin in solution, 500 nM Cry1Ab toxin was mixed with TBR peptides (100 nM), and immediately, after different time periods, aliquots of 100 μL of the incubated mixture were transferred to a previously coated 96-well ELISA plate with 2.5 μg of Cry1Ab toxin in coating buffer (50 mM sodium carbonate pH 9.6) to determine the amount of unbound TBR peptide as described (*44*). At the end of the kinetic analysis, the ELISA plate was washed three times and detected with anti-c-myc antibody (1:1000) coupled to a second anti-mouse coupled to HRP and detected by HRP enzymatic activity. To determine dissociation constants (K_d), TBR peptides (10 nM) were equilibrated with increasing concentrations of Cry1Ab toxin (ranging from 1 nM to 1 μM) in a 100 μL volume for 1 h at room temperature. The incubation mixture were transferred to a 96-well ELISA plate previously coated with 2.5 μg of Cry1Ab toxin and processed as above. The concentration of Cry1Ab toxin at which the half-maximal ELISA signal is detected corresponds to the dissociation constant (*45*).

Midgut Juice Isolation and Proteolytic Activation of Cry1Ab Protoxin. M. sexta larvae were reared on an artificial diet. Midgut tissue was dissected from the fifth instar larvae. Midgut juice was separated from solid material by centrifugation and filtered through 0.22 μm filters. For activation, 2 μg of Cry1Ab crystals was incubated for 1 h with a 1:4 ratio of scFv73, TBR1, or TBR2; midgut juice (5%) was added and incubated for 1 h at 37 °C. PMSF (1 mM) was added, and samples were centrifuged (20 min at 12 000*g*) as described (*28*).

Analysis of Hydropathic Profiles. A computer program described previously (hydropathie) (*46*, *47*) was used to compare hydropathic profiles of protein sequences. Five to 12 amino acid residue sequences with an opposed or similar hydropathic profile as the sequence query are selected by the software. Results are quantified through linear regression analysis of hydropathic values (Kyte and Doolittle scale) for a given position in each sequence.

RESULTS

Loops 2 and α-8 of Cry1Ab Toxin Have Similar Binding Capabilities. In previous work, we demonstrated that the CDR3 region of the scFv73 monoclonal antibody recognized domain II loop 2 of Cry1Aa and Cry1Ab toxins (*31*). Synthetic peptides with amino acid sequences corresponding to loop 2 or to scFv73 CDR3 competed with the binding of scFv73 to the Cry1A toxins in contrast to synthetic peptides corresponding to loops 1 and 3 or a scramble peptide of scFv73 CDR3 (*31*). Mutagenesis of loop α-8 showed that

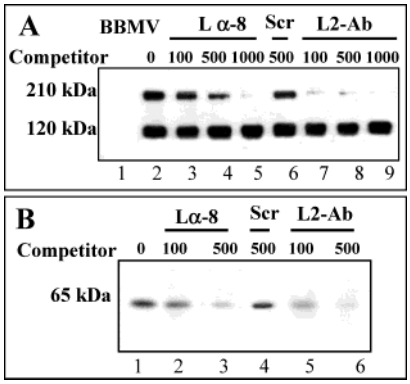

FIGURE 1: Cry1Ab domain II α-8 and 2 loops have similar binding capabilities. (A) Toxin overlay assays of Cry1Ab toxin to *M. sexta* BBMV. Lane 1, BBMV proteins without Cry1Ab binding; lane 2, BBMV with Cry1Ab toxin; lanes 3−5, same as lane 2 but competed with Lα-8 peptide; lane 6, same as lane 2 but competed with peptide Scr; and lanes 7−9, same as lane 2 but competed with L2-Ab peptide. (B) Western blot of trypsin activated Cry1Ab toxin. Lane 1, detected with scFv73; lanes 2 and 3, detected with scFv73 but competed with synthetic peptides Lα-8; lane 4, scFv73 detection competed with peptide Scr; and lanes 5 and 6, detected with scFv73 competed with L2-Ab peptide. Numbers in the upper part are molar excess of peptides used for competition.

this loop region is important for receptor interaction (*38*). We analyzed that a synthetic peptide with an amino acid sequence corresponding to loop α-8 (Lα-8) could compete with the binding of the Cry1Ab toxin to Bt-R_1 in a toxin overlay assay and to scFv73 in Western blots. Figure 1A shows a toxin overlay assay of blotted *M. sexta* brush border membrane vesicles (BBMV) showing that the Cry1Ab toxin can interact with two proteins of 120 kDa (APN) and of 210 kDa (Bt-R_1) as has been previously reported (*30*, *31*). The synthetic peptide Lα-8 competed with the binding of the Cry1Ab toxin to Bt-R_1 but not to APN. In contrast, the scramble peptide of scFv73 CDR3 (Scr) did not compete with the binding of Cry1Ab to Bt-R_1 (Figure 1A). Figure 1A shows that the loop 2 synthetic peptide (L2-Ab) competed more efficiently with the binding of Cry1Ab to Bt-R_1 than Lα-8 synthetic peptide. The Western blot of the Cry1Ab toxin revealed with scFv73 showed that the synthetic peptide Lα-8 competed with the binding of scFv73 to Cry1Ab as an L2-Ab synthetic peptide (Figure 1B). This result shows that loops 2 and α-8 have similar binding capabilities despite the fact that they share no amino acid sequence similarity.

Loops 2 and α-8 Bind to Different Regions in Bt-R_1. Previous work demonstrated that the Cry1Ab loop 2 region binds the ^{865}NITIHITDTNNK^{876} Bt-R_1 epitope (*31*). We decided to study Cry1Ab binding to the two characterized Cry1A binding regions to determine the amino acid residues of Cry1Ab involved in these interactions.

Two Bt-R_1 70 amino acid peptides were cloned by RT-PCR as reported in the Experimental Procedures. The first Bt-R_1 truncated peptide included residues 831−900 (TBR1) and contained epitope ^{865}NITIHITDTNNK^{876}. The second fragment comprised residues 1291−1360 and corresponds to the toxin binding region (TBR2) characterized by Dorsch et al. (*27*). The PCR products corresponding to these gene regions were sequenced and cloned in a vector containing a His-tag to facilitate their purification and a c-myc tag to facilitate their identification by anti-c-myc antibodies. After nickel-agarose purification from *E. coli* cells, two peptides

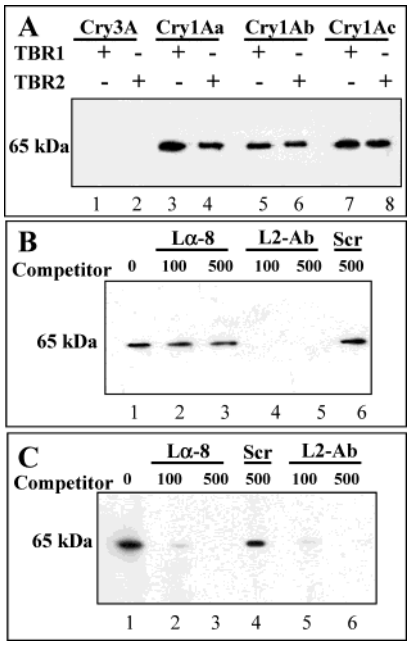

FIGURE 2: Bt-R_1 TBR1 region binds loop 2 and TBR2 binds loop α-8 and loop 2 of Cry1Ab toxin. (A) Blot detection of Cry3A (lanes 1 and 2), Cry1Aa (lanes 3 and 4), Cry1Ab (lanes 5 and 6), and Cry1Ac (lanes 7 and 8) with toxin binding regions TBR1 (lanes 1, 3, 5, and 7) and TBR2 (lanes 2, 4, 6, and 8). (B) Blot detection of Cry1Ab toxin with TBR1. Lane 1, without peptide competitors; lanes 2 and 3, Cry1Ab detection with TBR1 competed with synthetic peptide Lα-8; lanes 4 and 5, Cry1Ab detection with TBR1 competed with L2-Ab; lane 6, Cry1Ab detection with TBR1 competed with Scr peptide. (C) Blot detection of Cry1Ab with TBR2. Lane 1, without peptide competitors; lanes 2 and 3, Cry1Ab detection with TBR2 competed with synthetic peptide Lα-8; lane 4, Cry1Ab detection with TBR2 and competed with peptide Scr; lanes 5 and 6, Cry1Ab detection with TBR2 and competed with L2-Ab. Numbers in the upper part are molar excess of peptides used for competition.

of 10 kDa were obtained as revealed by a Western blot using anti-c-myc antibody (data not shown). Different Cry toxins were separated by SDS−PAGE, blotted onto nitrocellulose membranes, and detected with the two TBR regions revealed afterward with anti-c-myc antibody (see Experimental Procedures). Figure 2A shows that both TBR regions bind Cry1Aa, Cry1Ab, and Cry1Ac toxins in contrast to Cry3A, nontoxic to *M. sexta*, that showed no observed binding to any of the Bt-R_1 TBR regions.

To determine what loop regions of Cry1Ab toxin are involved in the interaction with the two TBR peptides, heterologous binding competition using synthetic peptides Lα-8 and L2-Ab were performed. Figure 2B shows that the binding of the Cry1Ab toxin to the TBR1 peptide (residues 831−900) was competed by L2-Ab synthetic peptide but not by Lα-8 synthetic peptide. Binding of Cry1Ab toxin to the TBR2 region (residues 1291−1360) was competed by both synthetic peptides, L2-Ab and Lα-8 (Figure 2C). The Scr peptide did not compete with the binding of Cry1Ab to the TBR fragments (Figure 2B,C).

Loop 2 Mutants Are Affected by Binding to TBR1 But Not to TBR2 Region. Several Cry1A mutants in loop 2 are affected by receptor binding and toxicity (*32*, *33*, *38*). To distinguish if loops 2 or α-8 bind to TBR2, we analyzed the binding of loop 2 mutants F371A, affected on irreversible binding (*32*, *33*), and RR368-9EE, affected on reversible

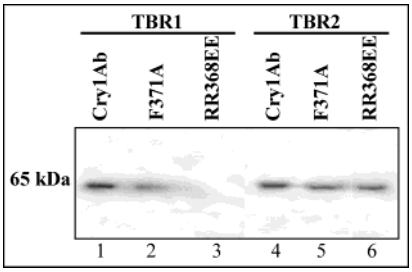

FIGURE 3: Binding of Cry1Ab loop 2 mutants to the two Bt-R_1 toxin binding regions. Blot detection of Cry1Ab toxin (lanes 1 and 4), F371A mutant (lanes 2 and 5), and RR368-9EE mutant (lanes 3 and 6) with TBR1 (lanes 1−3) or with TBR2 (lanes 4−6).

binding (*38*), to the two TBR regions. Figure 3 shows that the F371A mutant bound the two TBR regions, although it had a weaker binding to TBR1 than to TBR2. In contrast, mutant RR368-9EE showed no observable binding to the TBR1 region but still retained binding to TBR2. These results suggest that the Cry1Ab toxin binds TBR1 with loop 2 and TBR2 with loop α-8.

Cry1Ab Toxin Interacts with Bt-R_1 Epitope ^{1331}IPLPASILTVTV^{1342}. As shown in Figure 2C, the TBR2 fragment could interact with loops 2 and α-8, while TBR1 only interacts with loop 2 (Figure 2B). Accumulating evidence indicates that proteins can interact through amino acid sequences displaying inverse hydropathic profiles leading to the concept of hydropathic complementarity (*34*). We screened the TBR2 amino acid sequence, by computer assisted analysis, with both loops 2 and α-8 amino acid sequences searching for an amino acid sequence with a complementary hydropathic profile to both loop sequences. Figure 4 shows that the Bt-R_1 amino acid sequence ^{1331}IPLPASILTVTV^{1342} shows significant hydropathic complementarity to loop 2 ($r = 0.93$) and to loop α-8 ($r = 0.72$).

To determine if this amino acid sequence was responsible for Cry1Ab binding, we synthesize synthetic peptides with amino acid sequences corresponding to ^{1331}IPLPASILTVTV^{1342} (peptide EpTBR2) and to a sequence obtained from TBR2 but that does not share any sequence hydropathic complementarity to the loops 2 and α-8 regions (^{1296}LDPVRNRLFLKK^{1307}, peptide NonEpTBR2) to compete with the binding of the Cry1Ab toxin to the TBR2 fragment. Figure 5A shows that synthetic peptide EpTBR2 competed with the binding of Cry1Ab to TBR2 in contrast with peptide NonEpTBR2 or to peptide Scr. Figure 5B shows that synthetic peptides BtR1-Cry (corresponding to epitope ^{868}HITDTNN^{875}) as well as peptide EpTBR2 competed with the binding of Cry1Ab to Bt-R_1 in toxin overlay assays, but not to APN, in contrast to the scramble peptide or peptide NonEpTBR2.

Determination of Dissociation Constants by Analysis of Cry1Ab Toxin Interaction with TBR Peptides in Solution. To obtain quantitative data on the interaction of the Cry1Ab toxin with the two Bt-R_1 toxin binding regions, we analyzed the interaction of the toxin with the two TBR peptides in solution using a competition enzyme-linked immunosorbent assay (ELISA) (*44*). In this methodology, the association rate of Cry1Ab toxin and TBR peptides was measured by mixing both molecules in solution, and at different time intervals aliquots were withdrawn to determine by indirect ELISA the amount of free TBR peptide that remained in solution. The

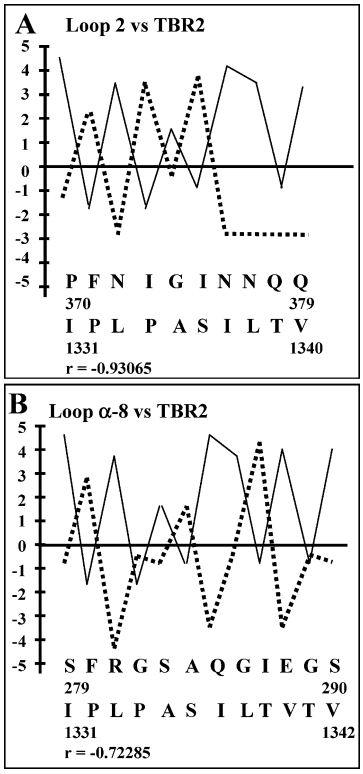

FIGURE 4: Identification of IPLPASILTVTV amino acid sequence by comparison of the hydropathic profiles of (A) loop 2 of Cry1Ab toxin (dotted line) and (B) loop α-8 (dotted line) of Cry1Ab toxin with the complete TBR2 amino acid sequence.

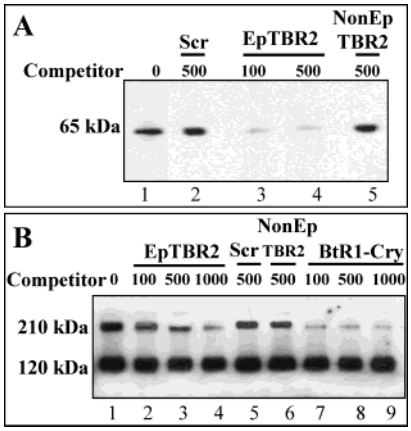

FIGURE 5: Cry1Ab toxin binds ^{1331}IPLPASILTVTV^{1342} Bt-R_1 amino acid sequence in TBR2 region. (A) Blot detection of Cry1Ab toxin with TBR2. Lane 1, without peptide competitors; lane 2, Cry1Ab detection with TBR2 competed with peptide Scr; lanes 3 and 4, Cry1Ab detection with TBR2 competed with EpTBR2 peptide; lane 5, Cry1Ab detection with TBR2 competed with NonEpTBR2 peptide. (B) Toxin overlay assay of *M. sexta* BBMV with Cry1Ab toxin. Lane 1, without competitor; lanes 2−4, Cry1Ab overlay assay competed with peptide EpTBR2; lane 5, competed with Scr peptide; lane 6, competed with NonTEpTBR2 peptide; lanes 7−9 competed with BtR1-Cry peptide. Numbers in the upper part are molar excess of peptides used for competition.

disappearance of free TBR peptide reflects the time course of the association reaction (*44*). To have a pseudo-first-order reaction, the concentration of the TBR peptide was at least 5-fold lower than the concentration of Cry1Ab toxin in solution. Also, the concentration of the Cry1Ab toxin in solution was more than 10-fold higher than the reported K_d value for TBR2 peptide (*27*). Figure 6 shows the kinetics of

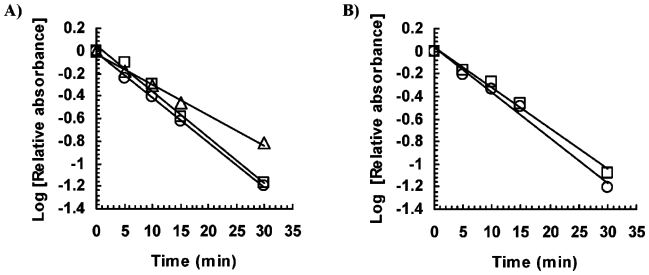

FIGURE 6: Kinetics of association of 500 nM Cry1Ab toxin (A) or 500 nM RR368-9EE mutant (B) to 40 nM TBR1 (△), 100 nM TBR2 (□), or 100 nM scFv73 (○). No detectable binding of RR368-9EE mutant to TBR1 peptide was observed. Plots are logarithm of relative absorbance vs time. The pseudo-first-order rate constant k_{obs} is given by the slope of the straight line. Relative absorbance represents the ratio $(A_t - A.)/(A_0 - A.)$, where A. is the ELISA signal on completion of the reaction, A_t the signal at time t, and A_0 the signal at time zero.

Table 2: Binding Kinetics of Cry1Ab and Mutant RR368-9EE to scFv73 and TBR Peptides[a]

	Cry1Ab		RR368-9EE	
peptide	k_{on} ($\times 10^5$ M^{-1} s^{-1})	K_d ($\times 10^{-8}$ M)	k_{on} ($\times 10^5$ M^{-1} s^{-1})	K_d ($\times 10^{-8}$ M)
TBR1	0.5	0.6	NBD[b]	NBD
TBR2	1	4.0	0.8	8.0
scFv73	1	3.6	0.7	7.5

[a] Binding kinetics was determined by competition ELISA as described in the Experimental Procedures. [b] NBD: no binding detected.

association of the two TBR peptides to Cry1Ab and the loop 2 RR368-9EE mutant. The plot is the logarithm of relative absorbance versus time where the slope of the line suggests a pseudo-first-order rate constant of association (k_{obs}). The association constant k_{on} was obtained by dividing the k_{obs} constant by the concentration of the Cry1Ab toxin and is shown in Table 2. Figure 6 shows that the Cry1Ab toxin binds the TBR1 peptide with higher affinity than TBR2 in contrast to the loop 2 RR368-9EE mutant that lost all binding to the TBR1 peptide and still interacts, although less efficiently, with the TBR2 peptide in agreement also with data obtained with the toxin blots revealed with the two TBR peptides (Figure 3). To determine the dissociation constants, TBR peptides were incubated in solution with a different excess of Cry1Ab toxin (1 nM to 1 μM), and the unbound TBR peptides were detected afterward with Cry1Ab toxin by ELISA. As a control, we determined also the dissociation constant of the scFv73 antibody to Cry1Ab toxin that has a K_d of 40−55 nM determined by surface plasmon resonance (*30*, *31*). Table 2 shows the k_{on} and K_d values obtained by competition ELISA showing that the affinity of Cry1Ab toxin to scFv73 and TBR2 is in agreement with previously published results (*27*, *30*, *31*). The data presented in Table 2 also shows that Cry1Ab toxin binds to the TBR1 peptide with a 6-fold higher affinity than to the TBR2 peptide. Also, the Cry1Ab RR368-9EE mutant had a 2-fold higher K_d value for binding to the TBR2 peptide than the Cry1Ab toxin.

Cry1Ab Pre-Pore Formation Induced by TBR Binding. Binding of the Cry1Ab toxin to scFv73 antibody facilitated the proteolytic cleavage of helix α-1 of domain I and the formation of a tetramer pre-pore of 250 kDa that is membrane insertion competent (*28*). To analyze the role of the binding of Cry1Ab to the two Bt-R_1 TBR regions on the formation

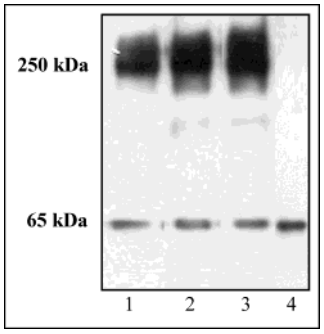

FIGURE 7: Binding of Cry1Ab protoxin to Bt-R_1 toxin binding regions TBR1 and TBR2 facilitates pre-pore oligomer formation. Western blot of Cry1Ab toxin after 1 h incubation with different peptides and proteolytic activated with *M. sexta* midgut juice detected with polyclonal anti-Cry1Ab antibody. Lane 1, proteolytic activation in the presence of scFv73; lane 2, activation in the presence of TBR2; lane 3, activation in the presence of TBR1; and lane 4, activated with midgut juice in the absence of the Bt-R_1 receptor or TBR peptides from the receptor.

Table 3: Toxicity of Cry1Ab Protein to *M. sexta* Larvae in the Presence or Absence of Competitors

treatment	mortality[a]
Cry1Ab[b]	96
Cry1Ab + scFv45 500X[c]	77
Cry1Ab + scFv45 1000X	81
Cry1Ab + scFv73 500X	42
Cry1Ab + scFv73 1000X	25
Cry1Ab + TBR1 500X	39
Cry1Ab + TBR1 1000X	29
Cry1Ab + TBR2 500X	25
Cry1Ab + TBR2 1000X	16
Cry1Ab + Mix (EpTBR1 + BtR1-Cry) 150X	14
Cry1Ab + Mix (EpTBR1 + BtR1-Cry) 300X	20
Cry1Ab + Scr 500X	95
control	0

[a] Percentage of 48 larvae per treatment. Representative results of three experiments. [b] 9 ng/cm^2 of toxin. [c] Molar excess of competitor.

of the 250 kDa pre-pore oligomer, proteolytic activation of the Cry1Ab protoxin with *M. sexta* midgut juice in the presence of the TBR peptides was performed, and the formation of the 250 kDa oligomer was analyzed by Western blot. Figure 7 shows that the binding of Cry1Ab to both TBR regions, as a scFv73 antibody, promoted the formation of the 250 kDa oligomer.

Involvement of TBR Regions of Bt-R_1 in Cry1Ab Toxicity. To determine if the TBR regions interfere with Cry1Ab toxicity to *M. sexta* larvae, bioassays were performed using the different TBR regions or peptides BtR1-Cry or EpTBR2 in combination with the Cry1Ab toxin. First, instar larvae were fed with Cry1Ab toxin either alone or with the Cry1Ab toxin previously incubated with a different fold molar excess of the different competitors. Table 3 shows that the toxicity of the Cry1Ab toxin was greatly reduced (up to 80%) when the toxin was incubated with scFv73 antibody, TBR1 peptide, TBR2 peptide, or synthetic peptides BtR1-Cry or EpTBR2 in contrast to antibody scFv45, which binds Cry1Ab toxin but does not affect receptor interaction (*30*), or peptide Scr.

DISCUSSION

Identification of the receptor binding epitopes of Cry toxins will be important for the characterization of resistant insect populations in nature and to develop strategies to design

toxins that could overcome receptor point mutations leading to Cry toxin resistance. Mutagenesis of Cry1A toxins revealed that loops 2, 3, and α-8 of domain II are involved in receptor recognition (*32*, *33*, *35*−*38*). In previous works, we identified the Bt-R_1 receptor epitope recognized by loop 2 of domain II of Cry1A toxins (*30*, *31*). In this paper, we narrowed to 12 amino acids another previously identified Bt-R_1 epitope (*27*) and identified loop α-8 of the Cry1Ab domain II as its cognate binding epitope.

Previous work demonstrated that loops 1 and 3 synthetic peptides did not compete with Cry1Ab binding to the Bt-R_1 in toxin overlay assays in contrast to loop 2 (*31*) and loop α-8 (Figure 1A). To determine the binding epitope in Bt-R_1 involved in the interaction with loop α-8, we cloned two 70 amino acid toxin binding regions, one containing the ^{865}NITIHITDTNN^{875} epitope identified by us (TBR1, residues 831−900) (*31*) and another identified by the heterologous expression of truncated derivatives of Bt-R_1 (TBR2, residues 1291−1360) (*27*). A synthetic peptide corresponding to loop 2 competed with the binding of Cry1Ab toxin to TBR1, while the loop α-8 synthetic peptide had no effect on this interaction, and the loop 2 mutation RR-368-9EE abolished the interaction of the Cry1Ab toxin to TBR1. These data confirm our previous results: loop 2 interacts with the ^{865}NITIHITDTNN^{875} epitope (*31*). Cry1Ab binding to TBR2 was competed by loops 2 and α-8. This result shows that loops α-8 and 2 can interact with the TBR2 region. Cry1Ab loop 2 mutant RR368-9EE retained the interaction with the TBR2 region. This result suggests that loop α-8 interacts with TBR2.

Domain II loop α-8 has similar binding capabilities as does loop 2 since synthetic peptides with amino acid sequences corresponding to these regions competed with the binding of a monoclonal scFv73 antibody to Cry1Ab toxin (Figure 1B) and with the binding of the toxin to the TBR2 region (Figure 2C). In several antibody−antigen interactions, it has been observed that several CDR regions have similar binding capabilities because of similar hydropathic patterns (*46*, *48*). The significance of antibodies with binding epitopes with similar binding capacities remains unclear but could be important to the binding mechanism. In antibody−antigen interactions, it has been suggested that similar binding CDR regions could imply a sequential binding mechanism (*48*−*50*). In the case of the Cry1Ab toxin, we cannot exclude the possibility that loops 2 and α-8 could interact with TBR2 in a sequential manner. In this regard, the binding affinity of the loop 2 mutant RR368-9EE to the TBR2 peptide was 2-fold lower than that of the Cry1Ab toxin suggesting that although the TBR2 peptide interacts with loop α-8, loop 2 is probably involved in the initial interaction with this region.

Regarding the interaction of loop 2 with the TBR1 region, work done by Dorsch et al. (*27*) showed that the Bt-R_1 truncated derivatives that contained the ^{865}NITIHITDTNN^{875} epitope did not bind the Cry1Ab toxin (*27*). This result is somehow surprising, although the Cry1Ab toxin binds the TBR1 region with a 6-fold higher affinity than to TBR2 as revealed by competition ELISA analysis (Table 2, Figure 6). In this paper, we show that a 70 amino acid truncated derivative of Bt-R_1 containing epitope ^{865}NITIHITDTNN^{875} was able to bind Cry1A toxins but not Cry3A (Figure 2A). One plausible explanation for the lack of binding of the Cry1A toxin to the TBR1 region in the context of larger Bt-R_1 truncated derivatives could be that in the latter context the ^{865}NITIHITDTNN^{875} epitope is occluded and not accessible for toxin binding. A sequential binding hypothesis could imply that the binding of the Cry1Ab toxin to the TBR2 region may induce a conformational change in the receptor, making the TBR1 epitope accessible for loop 2 interaction. Further experiments are needed to support a sequential binding interaction of loop regions of the Cry1Ab toxin with the two TBR regions in Bt-R_1. In the case of the closely related Cry1Ac toxin, a sequential binding mechanism to the APN receptor has been proposed (*37*). The interaction of domain III with a *N*-acetyl galactosamine moiety in the receptor precedes the binding of the loop regions of domain II (*37*).

It is generally accepted that the toxic effect of Cry proteins is exerted by the formation of a lytic pore. However, it has also been shown that the Cry1A toxins target cadherin-like molecules presumably involved in cell−cell interactions within susceptible hosts as is the case of several other pathogens (*27*). The disruption of the epithelial barrier may result from the targeting of cell junction molecules, besides the formation of pores. In this regard, it is remarkable that Cry1A toxins interact with at least two structural regions that are not close together in the primary sequence of Bt-R_1. Although we cannot exclude that both sites could be located nearby in the three-dimensional structure of Bt-R_1, it is tempting to speculate that the binding of Cry1A toxins could cause a conformational change in the cadherin molecule that could have a consequence with the interaction with other cell-adhesion proteins and consequently on the disruption of the epithelial cell layer.

The amino acid sequence of TBR2 involved in the Cry1Ab interaction was narrowed to 12 amino acids, ^{1331}IPLPASILTVTV^{1342}. This region was identified by searching for an amino acid region in TBR2 with a complementary hydropathic pattern to loops 2 and α-8 amino acid sequences. Competition experiments using peptide IPLPASILTVTV confirmed that this amino acid region was enough to compete with the binding of the Cry1Ab toxin to Bt-R_1 and to TBR2. This result shows that loop α-8 interacts with the Bt-R_1 epitope ^{1331}IPLPASILTVTV^{1342}. The TBR2 peptide or peptide ^{1331}IPLPASILTVTV^{1342} interfered with the toxicity of the Cry1Ab toxin showing that this is an important binding event involved in the interaction of the toxin to Bt-R_1.

In previous work, we demonstrated that the binding of Cry1Ab toxin to Bt-R_1, using scFv73 as surrogate of the receptor, facilitates proteolytic cleavage of helix α-1 and the formation of a pre-pore structure (*28*). Since the scFv73 antibody is able to interact with the two exposed loops α-8 and 2, we analyzed the effect of binding to the two TBR regions on the formation of the pre-pore structure. Both TBR regions promoted the proteolytic formation of the pre-pore (Figure 7). These results suggest that the interaction of the domain II loop regions with the Bt-R_1 receptor is a key step in the process of proteolytic activation of the toxin and the formation of the pre-pore oligomer. The interaction of domain II loop regions with the receptor may produce a conformational change in the toxin leading to the proteolytic processing of helix α-1 in domain I exposing a hydrophobic surface involved in toxin oligomerization.

In previous work, we showed that the interaction of loop 2 with the ^{865}NITIHITDTNNK^{876} Bt-R_1 epitope was deter-

mined by hydropathic complementarity (*31*). In the case of loop α-8, we show here that its interaction with the ^{1331}IPLPASILTVTV^{1342} Bt-R_1 epitope is also determined by hydropathic complementarity. Our results suggest that the analysis of hydropathic patterns of interacting epitopes of Cry toxins with their cognate receptor epitopes could offer tools for improving or changing specificities of Cry toxins.

ACKNOWLEDGMENT

The authors thank Dr. Jean-Yves Couraud (Gif-sur-Yvette, France) for the software to search hydropathic similarities or complementarities; Dr. Sarjeet S. Gill for helpful discussions; and Lizbeth Cabrera, Jorge F. Sanchez, and Claudia Morera for technical assistance. I.G. acknowledges CONACyT for a Ph.D. fellowship.

REFERENCES

1. Pietrantonio, P. V., and Gill, S. S. (1996) in *Biology of the Insect Midgut* (Lehane, M. J., and Billingsley, P. F., Eds.) pp 345−372, Chapman and Hall, London.
2. Li, J., Carroll, J., and Ellar, D. J. (1991) *Nature 353*, 815−821.
3. Grochulski, P., Masson, L., Borisova, S., Pusztai-Carey, M., Schwartz, J. L., Brousseau, R., and Cygler, M. (1995) *J. Mol. Biol. 254*, 447−464.
4. Morse, R. J., Yamamoto, T., and Stroud, R. M. (2001) *Structure 9*, 409−417.
5. Chen, X. J., Lee, M. K., and Dean, D. H. (1993) *Proc. Natl. Acad. Sci. U.S.A. 90*, 9041−9045.
6. Wolfersberger, M. G., Chen, X. J., and Dean, D. H. (1996) *Appl. Environ. Microbiol. 62*, 279−282
7. Schwartz, J. L., Potvin, L., Chen, X. J., Brousseau, R., Laprade, R., and Dean, D. H. (1997) *Appl. Environ. Microbiol. 63*, 3978−3984.
8. Schnepf, E., Crickmore, N., Van Rie, J., Lereclus, D., Baum, J. R., Feitelson, J., Zeigler, D., and Dean, D. H. (1998) *Microbiol. Mol. Biol. Rev. 62*, 705−806.
9. DeMaagd, R. A., Bravo, A., and Crickmore, N. (2001) *Trends Genet. 17*, 193−199.
10. Oppert, B., Kramer, K. J., Johnson, D. E. MacIntosh, S. C., and McGauhey, W. H. (1994) *Biochem. Biophys. Res. Comm. 198*, 940−947.
11. Lee, M, K., Rajamohan, F., Gould, F., and Dean, D. H. (1995) *Appl. Environ. Microbiol. 61*, 3836−3842.
12. Gahan, L. J., Gould, F., and Heckel, D. G. (2001) *Science 293*, 857−860.
13. Griffits, J. S., Whitacre, J. L., Stevens, D. E., and Aroian, R. V. (2001) *Science 293*, 860−864
14. Darboux, I., Pauchet, Y., Castella, C., Silva-Filha, M. H., Nielsen-LeRoux, C., Charles, J.-F., and Pauron, D. (2002) *Proc. Natl. Acad. Sci. U.S.A. 99*, 5830−5835.
15. Ferré, J., and Van Rie, J. (2002) *Annu. Rev. Entomol. 47*, 501−533.
16. Garczynski, S. F., and Adang, M. J. (1995) *Insect Biochem. Mol. Biol. 25*, 409−415.
17. Knight, P. J. K., Crickmore, N., and Ellar, D. J. (1994) *Mol. Microbiol. 11*, 429−436.
18. Vadlamudi, R. K., Weber, E., Ji, I., Ji, T. H., and Bulla, L. A., Jr. (1995) *J. Biol. Chem. 270*, 5490−5494.
19. Nagamatsu, Y., Koike, T., Sasaki, K., Yoshimoto, A., and Furukawa, Y. (1999) *FEBS Lett. 460*, 385−390.
20. Yaoi, K., Kadotani, T., Kuwana, H., Shinkawa, A., Takahashi, T., Iwahana, H., and Sato, R. (1997) *Eur. J. Biochem. 246*, 652−657.
21. Gill, S. S., Cowles, E. A., and Francis, V. (1995) *J. Biol. Chem. 270*, 27277−27282.
22. Oltean, D. I., Pullikuth, A. K., Lee, H.-K., and Gill, S. S. (1999) *Appl. Environ. Microbiol. 65*, 4760−4766.
23. Schwartz, J.-L., Lu, Y.-J., Sohnlein, P., Brousseau, R. L., Masson, L., and Adang, M. J. (1997) *FEBS Lett. 412*, 270−276.
24. Lorence, A., Darszon, A., and Bravo, A. (1997) *FEBS Lett. 414*, 303−307.
25. Zhuang, M., Oltean, D. I., Gómez, I., Pullikuth, A. K., Soberón, M., Bravo, A., and Gill, S. S. (2002) *J. Biol. Chem. 277*, 13863−13872.
26. Jenkins, J. L., and Dean, D. H. (2000) *Genetic Engineering: Principles and Methods* (Setlow, J. K., Ed.) p 33−54, Plenum Press, New York.
27. Dorsch, J. A., Candas, M., Griko, N. B., Maaty, W. S. A., Midbo, E. G., Vadlamudi, R. K., and Bulla, L. A., Jr. (2002) *Insect Biochem. Mol. Biol. 32*, 1025−1036.
28. Gómez, I., Sánchez, J., Miranda, R., Bravo, A., and Soberón, M. (2002) *FEBS Lett. 513*, 242−246.
29. Rajagopal, R., Sivakumar, S., Agrawal, N., Malhotra, P., and Bhatnagar, R. K. (2002) *J. Biol. Chem. 277*, 46849−46851.
30. Gomez, I., Oltean, D. I., Gill, S. S., Bravo, A., and Soberón, M. (2001) *J. Biol. Chem. 276*, 28906−28912.
31. Gomez, I., Miranda-Rios, J., Rudiño-Piñera, E., Oltean, D. I., Gill, S. S., Bravo, A., and Soberón, M. (2002) *J. Biol. Chem. 277*, 30137−30143.
32. Rajamohan, F., Alcantara, E., Lee, M. K., Chen, X. J., Curtiss, A., and Dean, D. H. (1995) *J. Bacteriol. 177*, 2276−2282.
33. Rajamohan, F., Cotrill, J. A., Gould, F., and Dean, D. H. (1996). *J. Biol. Chem. 271*, 2390−0.2396.
34. Blalock, J. E. (1995) *Nature Med. 1*, 876−878.
35. Lee, M. K., Jenkins, J. L., You, T. H., Curtiss, A., Son, J. J., Adang, M. J., and Dean, D. H. (2001) *FEBS Lett. 497*, 108−112.
36. Rajamohan, F., Hussain, S.-R. A., Cotrill, J. A., Gould, F., and Dean, D. H. (1996). *J. Biol. Chem. 271*, 25220−25226.
37. Jenkins, J. L., Lee, M. K., Valaitis, A. P., Curtiss, A., and Dean, D. H. (2000) *J. Biol. Chem. 275*, 14423−14431.
38. Lee, M. K., Rajamohan, F., Jenkins, J. L., Curtiss, A., and Dean, D. H. (2000) *Mol. Microbiol. 38*, 289−298.
39. Arantes, O., and Lereclus, D. (1991) *Gene 108*, 115−119.
40. Carroll, J., Convents, D., Van Damme, J., Boets, A., Van Rie, J., and Ellar, D. J. (1997) *J. Invert. Pathol. 70*, 41−49.
41. Lee, M. K., Milne, R. E., Ge, A. Z., and Dean, D. H. (1992) *J. Biol. Chem. 267*, 3115−3121.
42. Wolfersberger, M., Lüthy, P., Maurer, A., Parenti, P., Sacchi, F. V., Giordana, B. and Hanozet, G. M. (1987) *Comp. Biochem. Physiol. 86A*, 301−308.
43. Chomczynski, P., and Sacchi, N. (1987) *Anal. Biochem. 162*, 156−159.
44. Hardy, F., Djavadi-Ohaniance, L., and Goldberg, M. E. (1997) *J. Immunol. Methods 200*, 155−159.
45. Dong, L., Chen, S., Bartsch, U., and Schachner, M. (2003) *Biochem. Biophys. Res. Comm. 301*, 60−70.
46. Boquet, D., Déry, O., Frobert, Y., Grassi, J., and Couraud, J. Y. (1995) *Mol. Immunol. 32*, 303−308.
47. Wijkhuisen, A., Sagot, M. A., Frobert, Y., Créminon, C., Grassi, J., Boquet, D., and Couraud, J. Y. (1999) *FEBS Lett. 447*, 155−159.
48. Sagot, M.-A., Wijkhuisen, A., Créminon, C., Tymciu, S., Frobert, Y., Turbica, I., Grassi, J., Couraud, J.-Y., and Boquet, D. (2000) *Mol. Immunol. 37*, 423−433.
49. Hanin, V., Déry, O., Boquet, D., Sagot, M. A., Créminon, C., Couraud, J. Y., and Grassi, J. (1997) *Mol. Immunol. 34*, 829−838.
50. Van Regenmortel, M. H. V. (1998) *J. Dispersion Sci. Technol. 19*, 1199−1219.

BI034440P